Advances in Machinery, Materials Science and Engineering Application
M. Chen et al. (Eds.)

doi:10.3233/ATDE220470

Asynchronous Longitudinal Vibration of the Wheelset System

Linping SUN [a], Zhongliang YANG [a,1], Weihua MA [a], Shihui LUO [a] and Bo WANG [a]
[a] *State Key Laboratory of Traction Power, Southwest Jiaotong University, Chengdu, 610031, China*

Abstract. The longitudinal flutter of the wheelset system has caused abnormal wear of the wheel-rail and stripping of the tread surface, resulting in complex dynamic problems of the locomotive. And asynchronous longitudinal vibration of the wheelset could bring about different wear problems of the left and right wheels when the wheelset system was in some non-ideal working conditions. The longitudinal vibration model of the wheelset considering the effect of bending moment is established to obtain the equivalent force, which can carry out the vibration response simulation analysis of the left and right wheels , meanwhile, the irrational influencing factors are discussed. The results show that the system is stable when the creep rates of the left and right wheels are lower than the critical creep rate, otherwise, it will produce self-excited vibration. The analysis of the influencing factors of self-excited vibration indicate that the larger displacement of the center of mass of the wheelset will lead to the larger dynamic load in the system, increasing the vibration amplitude of the wheel on the offset side. And the vibration amplitude and velocity of the one with smaller primary longitudinal stiffness will increase, while the other one wheel will decrease. However, the wheel eccentric load is almost no effect on the longitudinal vibration amplitude.

Keywords. Longitudinal vibration, adhesion curve, self-excited vibration, eccentric center of mass, longitudinal stiffness

1. Introduction

The wheel-rail rolling contact theoretical model has been established by Carter [1], kalker [2], Johnson-Vermeulen [3] and Thompson [4], whose studies have been widely used in dynamic software. The dynamic change of the friction force on the wheel-rail contact surface will induce the wheelset torsional and longitudinal coupled self-excited vibration, and the wheelset longitudinal vibration will in turn cause the longitudinal creep rate/force at the contact spot to change periodically, affecting the wear of the wheel-rail contact surface.

In the wheelset longitudinal vibration analysis, Luo [5], who first analyzed the longitudinal vibration of the wheelset, pointed out that the longitudinal vibration of the wheelset would aggravate the dynamic force of the wheel-rail and cause the abnormal wear of the tread surface, and successfully solved the actual engineering problem of the DF8B locomotive. The finding of Ma [6] showed that the mechanism of the longitudinal vibration of the wheelset, and believed that the track irregularity, the

[1] Zhongliang Yang, Corresponding Author, State Key Laboratory of Traction Power, Southwest Jiaotong University, Chengdu, 610031, China; E-mail: clbyzl@163.com.

shaking of the wheelset, and the running speed was the important factors to cause the longitudinal vibration. A 3-dof torsional vibration model considering the torsional stiffness of the axle was established by Xu [7], who was used to analyze the torsional self-excited vibration behavior of the left and right wheels under different adhesion conditions, and discussed the stability of the torsional vibration. The complete locomotive dynamics model was established by Wang [8], who analyzed the longitudinal vibration of the locomotive under the condition of wheelset eccentricity, and showed that when the center of mass is radially eccentric, the wheel-rail creep force saturation will cause torsional vibration and longitudinal vibration further affects the vertical stability of the vehicle. The wheel-rail contact model during longitudinal vibration was established by Liu [9], who was used to analyze the longitudinal vibration mechanism of wheel-rail contact under the conditions of small creep and large creep, and could explain the polygonal wear mechanism of vehicle tread very well. The research of Yao [10], who established the torsional-longitudinal coupling vibration model, demonstrated that the vibrating system is stable when the wheelset is coupled in not exceeding the critical creep rate. Haberzettl [11] analyzed the relationship between the longitudinal dynamic behavior of automobile suspension on ride comfort and controllability, and showed that longitudinal vibration on uneven roads has a greater impact on comfort.

The above studies basically consider the vibration in the longitudinal direction (synchronous vibration) of the wheelset system under ideal working conditions. Wheelset system components have different maintenance times due to differences in materials and workloads, but the same components are synchronously maintained from an economical point of view, Such as the turning repair of the left and right, however, it will cause asynchronous wear when the defect of the wheelset system. This study focuses on the analysis of the vibration difference between the left and right wheels caused by the eccentricity of the center of mass of the wheelset, inconsistent longitudinal stiffness of the primary system, and the eccentric load of the wheelset, providing a theoretical reference for the engineering application of the differential wear of the left and right wheels of the wheelset.

2. Establishment of Wheelset Longitudinal Vibration Model

2.1. Model of Wheelset Longitudinal Vibration

The longitudinal vibration of the left (right) wheel in the train wheelset can be simplified to the single-degree-of-freedom model in figure 1(a), it can be described as:

$$m_w\ddot{x} + c\dot{x} + kx = F_{\mathrm{r}} - F_{\mathrm{r0}} \tag{1}$$

Where: k_1 - primary longitudinal stiffness, c_1 - primary longitudinal damping, F_{r} - creep force, F_{r0} - creep force at equilibrium position, m_c -1/4 car body mass (Shaft type: $2B_0$) , m_w - left (right) wheel mass, r_0 - rolling circle radius, v - wheel translation speed, w - wheel roll angular velocity, x_w - displacement at equilibrium position.

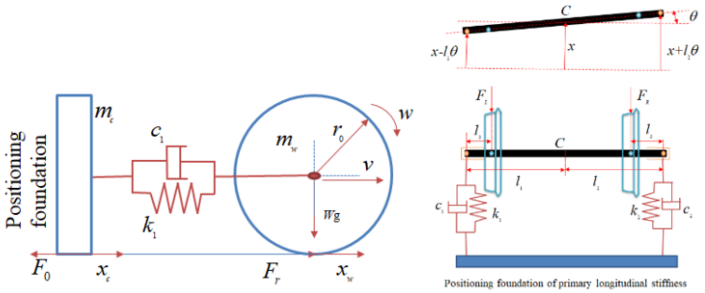

(a) Single Wheel Vibration (b) Wheelset vibration model

Figure 1. Longitudinal vibration model of wheelset.

Note the equivalent force on the right side of the vibration equation (the current creep force minus the creep force at the equilibrium position):

$$F_c(\dot{x}) = F_{\mathrm{r}} - F_{\mathrm{r0}} \tag{2}$$

Establish the longitudinal vibration model considering the bending moment of the wheelset as shown in figure 1(b), the differential equation of plane motion is established with the wheelset centroid point C to get the equation (ignoring the influence of weak damping):

$$\begin{bmatrix} m_w & 0 \\ 0 & I_w \end{bmatrix}\begin{bmatrix} \ddot{x}_C \\ \ddot{\theta}_C \end{bmatrix} + \begin{bmatrix} k_1+k_2 & k_2l_2-k_1l_1 \\ k_2l_2-k_1l_1 & k_1l_1^2+k_2l_2^2 \end{bmatrix}\begin{bmatrix} x_C \\ \theta_C \end{bmatrix} = \begin{bmatrix} F_L+F_R \\ F_L(l_1-l_3)-F_R(l_2-l_3) \end{bmatrix} \tag{3}$$

Where: F_L, F_R - equivalent force of left and right wheels, l_1 (l_2)- the distance from the longitudinal positioning stiffness of the left (right) wheel to the center of mass C, l_3 - the distance from primary longitudinal stiffness to the wheel.

It can be known from figure 1(b) that the vibration displacement expressions of the left and right wheels of the wheelset are:

$$\begin{aligned} x_L &= x_C - (l_1 - l_3)\theta_C \\ x_R &= x_C + (l_2 - l_3)\theta_C \end{aligned} \tag{4}$$

2.2. Calculation of Equivalent Force

The calculation of the equivalent force in formula (2) is related to the adhesion conditions of the wheel and rail and creep force and other parameters. And the forward traction force of the train is generated due to the creep effect between the wheel and rail, and its creep rate [12] is expressed as:

$$s = (\omega r_0 - \boldsymbol{v})/\omega r_0 = 1 - \boldsymbol{v}_0 + \dot{\boldsymbol{x}}/(\omega_0 + \dot{\theta})r_0 \tag{5}$$

Where: v_0 - wheelset average translation speed, ω_0 - wheelset average angular velocity, $\dot{x}$ - vibration component of wheelset translation, $\dot{\theta}$ - vibration component of wheelset rotation.

The formula (5) can be changed into (6) when considering only the vibration in the longitudinal direction (such as track irregularity and other factors) and ignoring the torsional vibration ($\dot{\theta}$=0),

$$s = 1 - \left(v_0 + \dot{x}\right) / \omega_0 r_0 \tag{6}$$

and the average slip rate $s_0 = 1 - v_0 / \omega_0 r_0$ can obtain when $\dot{x}$=0 .

Figure 2 is a simplified diagram of the wheel-rail adhesion characteristic curve, where the straight line OA is the positive slope segment, expressing as the wheel-rail adhesion area, where the straight line AB is the negative slope segment, expressing as the wheel-rail sliding area. Different adhesion curve parameters are set as OAB: s_m=0.02 , u_m=0.25 , k_u= -0.25 .

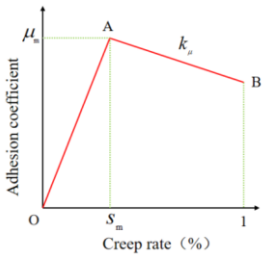

Figure 2. Simplified stick-slip characteristic curve.

The stick-slip characteristic curve OAB shown in figure 2 is expressed as a piecewise function:

$$\mu = \begin{cases} \mu_{\mathrm{m}} s / s_{\mathrm{m}} & 0 \le s < s_{\mathrm{m}} \\ \mu_{\mathrm{m}} + k_{\mu}\left(s - s_{\mathrm{m}}\right) & s_{\mathrm{m}} < s \le 1 \end{cases} \tag{7}$$

The instantaneous adhesive force between the wheel and rail is expressed as:

$$F_r = \mu W_0 \tag{8}$$

Where: W_0 - wheel load.

The expression for the available force $F_r\left(\dot{x}\right)$ can be obtained by substituting equation (7) into equation (8).

$$F_r\left(\dot{x}\right) = \begin{cases} \dfrac{\mu_{\mathrm{m}}}{s_{\mathrm{m}}} W_0 - \dfrac{\mu_{\mathrm{m}}\left(v_0 + \dot{x}\right)}{s_{\mathrm{m}} \omega_0 r_0} W_0 & 0 \le s < s_{\mathrm{m}} \\ \mu_{\mathrm{m}} W_0 + k_{\mu} W_0 \left(1 - \dfrac{v_0 + \dot{x}}{\omega_0 r_0} - s_{\mathrm{m}}\right) & s_{\mathrm{m}} \le s < 1 \end{cases} \tag{9}$$

The force at the initial equilibrium position can be obtained as following when $\dot{x}$=0

$$F_{r0}(\dot{x})=\begin{cases}\dfrac{\mu_{\mathrm{m}}}{s_{\mathrm{m}}}W_0-\dfrac{\mu_{\mathrm{m}}\boldsymbol{v}_0}{s_{\mathrm{m}}\omega_0 r_0}W_0 & 0\le s_0<s_{\mathrm{m}}\\ \mu_{\mathrm{m}}W_0+k_\mu W_0\left(1-\dfrac{\boldsymbol{v}_0}{\omega_0 r_0}-s_{\mathrm{m}}\right) & s_{\mathrm{m}}\le s_0<1\end{cases} \tag{10}$$

The equivalent force of the left and right wheels will be obtained by substituting equations (9) and (10) into equation (3).

(1) $s_0<s_m$, the average creep rate is located in the positive slope section of the adhesion coefficient curve:

$$F_c(\dot{x})=\begin{cases}-\dfrac{\mu_{\mathrm{m}}\dot{x}}{s_{\mathrm{m}}\omega_0 r_0}W_0 & 0\le s<s_{\mathrm{m}}\\ \mu_{\mathrm{m}}W_0(1-\dfrac{1}{s_m})+k_\mu W_0\left(1-\dfrac{\boldsymbol{v}_0+\dot{x}}{\omega_0 r_0}-s_{\mathrm{m}}\right)+\dfrac{\mu_{\mathrm{m}}\boldsymbol{v}_0}{s_{\mathrm{m}}\omega_0 r_0}W_0 & s_{\mathrm{m}}\le s<1\end{cases} \tag{11}$$

(2) $s_0>s_m$, the average creep rate is located in the negative slope section of the adhesion coefficient curve:

$$F_c(\dot{x})=\begin{cases}\mu_{\mathrm{m}}W_0(\dfrac{1}{s_m}-1)-\dfrac{\mu_{\mathrm{m}}(\boldsymbol{v}_0+\dot{x})}{s_{\mathrm{m}}\omega_0 r_0}W_0-k_\mu W_0\left(1-\dfrac{\boldsymbol{v}_0}{\omega_0 r_0}-s_{\mathrm{m}}\right) & 0\le s<s_{\mathrm{m}}\\ -k_\mu W_0\dfrac{\dot{x}}{\omega_0 r_0} & s_{\mathrm{m}}\le s<1\end{cases} \tag{12}$$

3. Longitudinal Vibration Simulation Analysis

Take the following parameters to simulate: r_0=0.625m , v_0=60km/h , W_0=12.5t , l_1=l_2=1.055m , k_1=k_2=36MN/m . The equivalent force $F_c(\dot{x})$ can be obtained through the left and right wheels by selecting the adhesion characteristic curves shown in figure 2. The MATLAB program is established to solve equation (3), in which the initial displacement and angular velocity are both zero, and the simulation process adds an excitation signal to the wheelset system to simulate the initial excitation of the system.

The phase plane response of the system is shown in figure 3 When s_0 takes different values, it can be concluded that the system will not generate self-excited vibration when s_0 is less than s_m, otherwise , it will generate self-excited vibration.

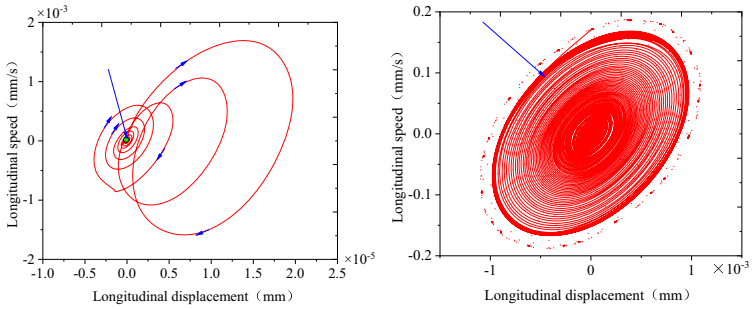

(a) s_0=0.01 (b) s_0=0.03

Figure 3. Phase plane of left (right) wheel.

It can be seen that there are many factors in the irrational working state of the left and right wheels from the longitudinal vibration model shown in figure 1. The asynchronous vibration under several main influencing factors is analyzed when the left and right wheels are both in the negative slope of the adhesion curve (s_0=0.03).

3.1. Eccentric Center of Mass of Wheelset

The longitudinal creep rate/force of the wheelset will change greatly when the radial center of mass of the wheelset is eccentric. Move the center of mass position C shown in figure 1 to the left by a certain distance (reduce l_1 and increase l_2) to simulate the center of mass of the wheelset radial eccentricity, figures 4(a-c) show the corresponding longitudinal dynamic analysis results of simulation analysis with offset values of 0mm, 10mm and 20mm.

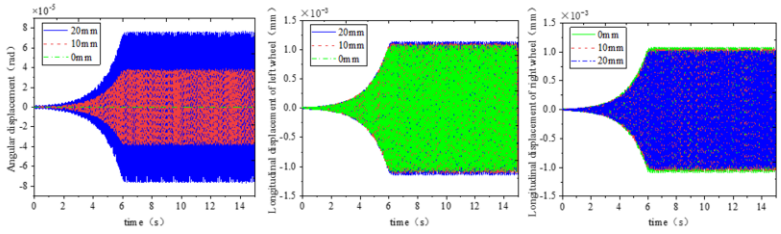

(a) Angular displacement of the centroid; (b) Amplitude of left wheel; (c) Amplitude of right wheel;

Figure 4. Longitudinal vibration response with eccentric center of mass.

It can be seen that the larger the displacement of the center of mass, the greater the vibration angular velocity of the axle from (a) and (b), the greater the vibration displacement of the left wheel, and the smaller the vibration displacement of the right wheel (c). Exploring reasons is that the eccentricity of the center of mass makes the dynamic potential energy (inertia) of the offset side during the vibration process greater, and the greater the offset value, the greater the vibration displacement.

3.2. Inconsistent Longitudinal Stiffness

In the long-term service of the vehicle, the longitudinal primary positioning structure will inevitably suffer from wear, aging and damage, leading to the change of the stiffness value. Using the wheelset longitudinal vibration model shown in figure 1, the wheelset vibration problem when the stiffness is inconsistent is simulated and analyzed by changing the value of the longitudinal stiffness k2 of the right wheel primary system, and the value of k2 is taken as a multiple of the left wheel k1: 1*k1, 0.9* k1, 0.8*k1, the longitudinal dynamic response of the wheelset is shown in figures 5(a-c).

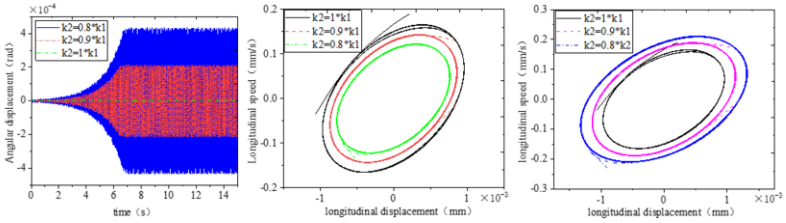

(a) Angular displacement of the centroid; (b) Left wheel phase plane; (c) Right wheel phase plane;

Figure 5. Longitudinal vibration response with inconsistent longitudinal stiffness.

It can be seen from (a) that the greater the difference in stiffness, the greater the swing angular displacement of the axle; Figures 5(b) and (c) show that as k2 decreases, the limit cycle formed by the vibration of the left wheel is smaller, while the limit cycle formed by the right wheel gradually increases, This is because the decrease in stiffness will lead to an increase in displacement under the condition of a certain adhesive force, and the vibration speed on the side of decreased stiffness will also increase due to the interconnection of the left and right wheels.

3.3. Wheel Weight Eccentric Load

The body load on the left and right wheels will be different due to factors such as the vehicle itself or the line (especially the curve line), which will lead to the difference in the adhesion of the left and right wheels. Under the condition that the total axle load is kept constant at 25t, the eccentric axle load is simulated with the revolver load shedding of 0t, 1t, and 2t. The longitudinal dynamic response is shown in figures 6(a-c).

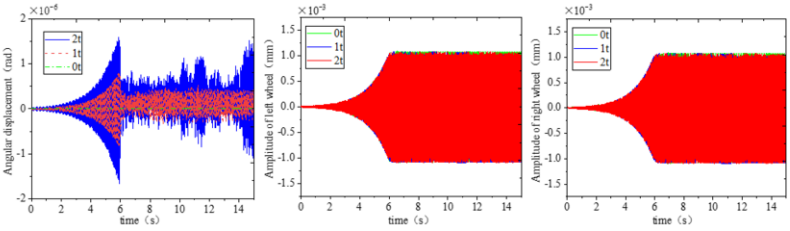

(a) Angular displacement of the centroid; (b) Amplitude of left wheel; (c) Amplitude of right wheel;

Figure 6. Longitudinal vibration response of wheelset under eccentric load.

It can be seen from figures 6(a), (b) and (c) that the vibration amplitude and speed of the left and right wheels are not much different. Figure 6(a) shows that the greater the eccentric load, the greater the angular velocity of the center of mass, but the magnitude of the rotational angular velocity is compared with figure 5(a) is much smaller, and it can be seen from equation (4) that the influence of the difference in vibration response of the left and right wheels is almost the same.

4. Conclusions

The longitudinal vibration model of the wheelset system is established to simulation analysis asynchronous vibration, and it shows that self-excited vibration will not occur when its adhesion lower than the critical value of the adhesion characteristic curve, otherwise, self-excited vibration will occur. The radial center of mass offset of the wheelset and the longitudinal stiffness of the primary system all affect the limit cycles of the left and right wheels when the longitudinal self-excited vibration of the wheelset occurs, However, the eccentric load of the wheel has little effect on the amplitude of the left and right wheels.

References

[1] Carter FW. On the action of a locomotive driving wheel. Proceedings of the Royal Society of London. Series A.1926 Aug; 112(760): 151-157.
[2] Kalker JJ. A fast algorithm for the simplified theory of rolling contact (FASTSIM program). Vehicle Systems Dynamics. 1982 Jul; 11(1): 1-13.
[3] Shen ZY, Hedrick JK, Elkins JA. A comparison of alternative creep force models for rail vehicle dynamic analysis. Vehicle System Dynamics, 1983 Jul; 12(1): 79-83.
[4] Wu TX, Thompson DJ. Wheel/rail non-linear interactions with coupling between vertical and lateral directions. Vehicle System Dynamics. 2004 Aug; 41(1): 27-49.
[5] Luo SH, Jin DC, Chen Q. Research on longitudinal vibration of wheelset and related problems of locomotive and rolling stock. Journal of Railways. 2005 Jun; 27(3):26-34.
[6] Ma WH, Luo SH. Influence of track irregularity on longitudinal vibration of wheelset and correlation performance. Journal of Southwest Jiaotong University. 2006 Sept; 14(3):238-251.
[7] Xu K, Zeng J, Wei L. An analysis of the self-excited torsional vibration of high-speed train drive system. Journal of Mechanical Science and Technology, 2019 Mar; 33(3):1149-1158.
[8] Wang C, Liu W, Ma WH. Influence of wheelset radial center of mass deviation on longitudinal vibration. Noise and Vibration Control. 2014 Feb; 34(1):41-43.
[9] Liu W, Ma WH, Luo SH. Research into the problem of wheel tread spalling caused by wheelset longitudinal vibration. Vehicle System Dynamic, 2015 Oct; 53: 546-567.
[10] Yao Y, Zhang HJ, Luo SH. An analysis of resonance effects in locomotive drive systems experiencing wheel/rail saturation adhesion. Proc. IMechE. Part F: J. Rail and Rapid Transit. 2014 Aug; 228(1):4-15.
[11] Haberzettl S, Zschocke AK, Gauterin F. A new method for studying the longitudinal dynamic behavior of a suspension on a test rig. Proceedings of the Institution of Mechanical Engineers, Part D. Journal of Automobile Engineering. 2016 Sept; 230(8):1027-1039.
[12] Frederich F. Kraftschlussbeansprung am schrag rollenden Schienen fahrzeuge. Glasers Annalen. 1970 Jun; 94(1):86-94.